

Resonance Raman, X-ray Crystallographic, and Magnetic Susceptibility Studies of Metal–Metal-Bonded MoRu and WOs Porphyrin Dimers. 1. Evidence for an Unusual MO Diagram

James P. Collman,^{*,†} S. T. Harford,[†] Stefan Franzen,^{‡,§} Jean-Claude Marchon,^{‡,||} Pascale Maldivi,^{||} Andrew P. Shreve,[‡] and William H. Woodruff[‡]

Department of Chemistry, Stanford University, Stanford, California 94305, Los Alamos National Laboratory, Los Alamos, New Mexico 87545, and Département de Recherche Fondamentale sur la Matière Condensée/SCIB, CEA-Grenoble, 38054 Grenoble, France

Received August 25, 1998

Solution (VT NMR, Evans method magnetic susceptibility, resonance Raman) and solid-state (SQUID magnetic susceptibility, X-ray crystallography) spectroscopic studies of intertriad heterodimeric [(OEP)MoRu(OEP)] (**1**), [(OEP)WOs(OEP)] (**2**), and [(OEP)MoRu(TPP)]PF₆ (**3**⁺) metalloporphyrins are reported (OEP = 2,3,7,8,12,13,17,18-octaethylporphyrinato; TPP = 5,10,15,20-tetraphenylporphyrinato). Solution and solid-state magnetic susceptibility data indicate that **1** and **2** contain two unpaired electrons in the ground electronic configuration. The presence of a δ bond in **3**⁺ has been confirmed by structural characterization. The experimental evidence is consistent with a molecular orbital ordering, $\sigma < \pi < \delta < \pi^* < \delta^*$, which is different from that seen for homologous metalloporphyrin dimers with homometallic or intratriad heterometallic multiple metal–metal bonds. Resonance Raman data suggest that the heterometallic bonds are slightly stronger than isoelectronic homometallic species.

Introduction

Recently, our laboratory has developed a procedure enabling the preparation and isolation of metal–metal-bonded dimers composed of transition metals from distinct triads in the periodic table.¹ Previously, the field of heterometallic transition metal–metal-bonded complexes had been limited to the study of bonds between metals from the same triad, CrMo, MoW, and RuOs.² This paper and the one immediately following are the first to develop our physical and chemical understanding of intertriad heterometallic bonds.

In this first paper we discuss various spectroscopic (variable-temperature ¹H NMR, resonance Raman, magnetic susceptibility, and X-ray crystallographic) studies of MoRu and WOs porphyrin dimers with the goal of determining a proper molecular orbital diagram. Since the Ru₂, Os₂, RuOs, Rh₂, Ir₂, Mo₂, W₂, MoW, and Re₂ porphyrin dimers have all been previously shown³ to be consistent with the traditional $\sigma\pi\delta\delta^*\pi^*\sigma^*$ molecular orbital ordering,⁴ it was reasonable to expect spectroscopic properties consistent with a $\sigma^2\pi^4\delta^2\delta^*2$ description for the d⁴–d⁶ metalloporphyrin dimers [(OEP)MoRu(OEP)] and [(OEP)WOs(OEP)]. However, metal–metal complexes with ligand systems other than porphyrins have been

shown to exhibit magnetic and structural properties consistent with several other molecular orbital descriptions (Cotton et al. have recently provided a very useful summary⁵ of these investigations). Thus, although the $\sigma\pi\delta\delta^*\pi^*\sigma^*$ description is the only one currently demonstrated for metalloporphyrin dimers, it is not the only metal–metal bond molecular orbital diagram with precedent.

Experimental Section

Materials. H₂OEP,⁶ H₂TPP,⁷ Mo(OEP)(PhC≡CPh),⁸ W(OEP)-(PEt₃)₂,⁹ Os(OEP or TPP)(pyridine)₂,¹⁰ and Ru(OEP or TPP)(pyridine)₂¹⁰ were synthesized according to methods described in the literature. Diethylpyrrole was donated by Pharmacyclics and distilled immediately prior to use. Cobaltocene and ferrocenium hexafluorophosphate were purchased from Strem and used as received. Benzene-*d*₆ and toluene-*d*₈ were purchased from Cambridge Isotope Laboratories and vacuum distilled from sodium benzophenone ketyl immediately prior to use. Solvents used for the metalation (decalin, chlorobenzene) and manipulation (benzene, toluene, hexanes, and dichloromethane) of the dimers were distilled from sodium benzophenone ketyl or P₂O₅ under argon before introduction into the glovebox.

Physical Measurements. A nitrogen-filled Vacuum Atmospheres drybox equipped with a Dri-Train inert gas purifier was employed for manipulations carried out under anaerobic conditions. ¹H NMR spectra were recorded on a Varian XL-400 or Varian-Inova 500 MHz FT-NMR spectrometer using benzene-*d*₆ or toluene-*d*₈ as a solvent.

[†] Stanford University.

[‡] Los Alamos National Laboratory.

[§] Current address: North Carolina State University, Raleigh, NC 27695.

^{||} CEA-Grenoble.

- (1) (a) Collman, J. P.; Arnold, H. J.; Weissman, K. J.; Burton, J. M. *J. Am. Chem. Soc.* **1994**, *116*, 9761–9762. (b) Collman, J. P.; Harford, S. T.; Marchon, J.-C.; Maldivi, P. *J. Am. Chem. Soc.* **1998**, *120*, 7999–8000.
- (2) Cotton, F. A.; Walton, R. A. *Multiple Bonds Between Metal Atoms*; 2nd ed.; Clarendon Press: Oxford, U.K., 1993; and references therein.
- (3) (a) Collman, J. P.; Arnold, H. A. *Acc. Chem. Res.* **1993**, *26*, 586–592. (b) Kadish, K.; Guillard, R. *Comments Inorg. Chem.* **1988**, *7*, 287–304.
- (4) (a) Figgis, B. N.; Martin, R. L. *J. Chem. Soc.* **1956**, 3837–3846. (b) Cotton, F. A. *Inorg. Chem.* **1965**, *4*, 334–336.

- (5) Cotton, F. A.; Yokochi, A. *Inorg. Chem.* **1997**, *36*, 567–570.
- (6) Sessler, J. L.; Mozaffari, A.; Johnson, M. R. *Org. Synth.* **1992**, *70*, 68–77.
- (7) Adler, A. D.; Longo, F. R.; Finarelli, J. D.; Goldmacher, J.; Assour, J.; Korsakoff, L. *J. Org. Chem.* **1966**, *32*, 476.
- (8) De Cian, A.; Colin, J.; Schappacher, M.; Ricard, L.; Weiss, R. *J. Am. Chem. Soc.* **1981**, *103*, 1850–1851.
- (9) Collman, J. P.; Garner, J. M.; Woo, L. K. *J. Am. Chem. Soc.* **1989**, *111*, 8141–8148.
- (10) Antipas, A.; Buchler, J. W.; Gouterman, M.; Smith, P. D. *J. Am. Chem. Soc.* **1978**, *100*, 3015–3024.

Resonances in the ^1H NMR were referenced versus the residual proton signal of the solvent.

Resonance Raman samples were prepared in a glovebox and flame sealed under vacuum in 5 mm Pyrex NMR tubes. Excitation for the RR experiments was provided by an Ar^+ ion laser (Spectra Physics). Typical laser powers were 20–30 mW on resonance. Scattered light was collected by an $f/1.5$ cm focal length lens and focused onto the slit of a SPEX 1877 0.6 m triple monochromator. Typical data acquisition times were 20 min. Because the precision of the depolarization ratios (ρ) was ± 0.1 , only general information such as whether bands were polarized (a_{1g} modes), depolarized (b_{1g} and b_{2g}), or anomalously polarized (a_{2g}) could be determined. NMR active species were studied in deuterated solvents, and sample integrity following excitation was confirmed by ^1H NMR. Cationic species were monitored by electronic absorption spectroscopy following UV excitation, and again no evidence for sample degradation was found.

Crystals of the [(OEP)MoRu(TPP)]PF₆ dimer (vide infra) suitable for X-ray diffraction were obtained by vapor diffusion of benzene into a saturated dichloromethane solution. A lustrous blue crystal with dimensions $0.10 \times 0.15 \times 0.32$ mm was chosen and mounted on a glass fiber in paratone N oil at -80 °C using an improvised cold stage. All measurements were made on a Siemens SMART diffractometer with graphite-monochromated Mo K α radiation. Cell constants and an orientation matrix for data collection, obtained from a least-squares refinement using the setting angles of 7767 carefully centered reflections with $I > 10\sigma(I)$ in the range $1.94^\circ < 2\theta < 49.50^\circ$, corresponded to a cell with dimensions $a = 17.5677(3)$ Å, $b = 42.8491(3)$ Å, $c = 21.0196(3)$ Å, $\beta = 90.613(1)^\circ$, $Z = 8$, and $V = 15821.8(3)$ Å³. The data were collected at a temperature of -104 °C using the ω scan technique to a maximum 2θ value of 49.5° .

The structure was solved by direct methods (SHELXS-86) and expanded using Fourier techniques (DIRDIF92). All Mo, Ru, P, F, and Cl atoms were refined anisotropically. Carbon and nitrogen atoms were refined isotropically. With hydrogen atoms included at idealized positions, the final cycle of full-matrix least-squares refinement (10 303 observed reflections with $I > 3\sigma(I)$ and 985 variable parameters) converged to $R = \sum||F_o| - |F_c||/\sum|F_o| = 0.080$ and $R_w = [(\sum w(|F_o| - |F_c|)^2)/\sum wF_o^2]^{1/2} = 0.093$.

Solid-state magnetic susceptibility measurements were performed under helium using a Quantum Design MPMS5 SQUID susceptometer. Measurements were taken using a field strength of 5000 G and were collected over a temperature range of 2–300 K. Each raw data file was corrected for the diamagnetic contribution of both the sample holder and the compound itself. A measured value of the molar susceptibility of H₂OEP (-481×10^{-6} cgs emu/mol) and tabulated values of metal ion susceptibilities¹¹ were used to calculate the diamagnetic correction (-1006×10^{-6} emu/mol) for **1**. The data were fit using a nonlinear least-squares regression program. The following parameters were varied: zero-field splitting, parallel and perpendicular g values, and the fraction of impurity.

Magnetic susceptibility of toluene-*d*₈ solutions of **1–3** were determined at ambient temperature by NMR spectroscopy according to the method outlined in ref 12. Tetramethylsilane and protiotoluene were used as a reference. A solution of 4.35 mg of **1** in 0.60 mL of toluene produced an average frequency shift of 7.5 Hz at an operating frequency of 400 MHz. Similarly, a solution of 4.51 mg of **2** in 0.65 mL of toluene produced an average frequency shift of 6.5 Hz also at an operating frequency of 400 MHz. A diamagnetic correction of -481×10^{-6} cgs emu/mol was applied to account for the porphyrin ligands.

Mass spectrometry was performed at the Mass Spectrometry Facility at the University of California at San Francisco and by Dr. Doris Hung of the Analytical Services Division at Northwestern University.

Preparation of [(OEP)MoRu(OEP)] (1). Vacuum pyrolysis of a mixture of Mo(OEP)(PhC \equiv CPh) (21.0 mg) and Ru(OEP)(py)₂ (22.3 mg) at 6×10^{-6} Torr and 210 °C (4 h) yields 32.4 mg of a mixture of 24% [Mo(OEP)]₂, 65% [(OEP)MoRu(OEP)], and 11% [Ru(OEP)]₂.

Oxidation. In a nitrogen-atmosphere glovebox, the reaction mixture is dissolved in benzene (7 mL), and to this is added Cp₂FePF₆ (4.4

mg, 13.3 μmol , 0.75 equiv relative to [(OEP)MoRu(OEP)]). The mixture is stirred overnight and then filtered through Celite. The precipitate is rinsed with benzene and then eluted with dichloromethane. The solution is concentrated under vacuum to yield [(OEP)MoRu(OEP)]-PF₆ (EPR, frozen toluene/dichloromethane, 1:1, 77 K: $g_{\parallel} = 1.973$, $g_{\perp} = 1.952$).

Reduction. To this solid is added an excess of Cp₂Co^{II} in benzene (5 mL) and stirred for 4 h. The solution is concentrated while heating under vacuum to remove unreacted Cp₂Co and side product Cp₂CoPF₆. The residual solid is [(OEP)MoRu(OEP)] (14.2 mg, 49.0%); neither of the homodimers are observed in either the ^1H NMR or mass spectrum.

UV-vis [nm (C₆H₆, log ϵ): Soret Ru(OEP) 366 (4.66), Soret Mo(OEP) 398 (4.86), 529 (4.16). ^1H NMR (ppm, C₆D₆): δ -30.90 (s, 4H, Mo H_{meso}); -8.10 (s, 4H, Ru H_{meso}); 9.10 (m, 8H, Mo-CH₂CH₃), 10.98 (m, 8H, Mo-CH₂CH₃); 5.20 (m, 8H, Ru-CH₂CH₃), 5.70 (m, 8H, Ru-CH₂CH₃); 0.55 (t, 24H, Mo-CH₂CH₃); 1.75 (t, 24H, Ru-CH₂CH₃). μ_{eff} (Evans method, toluene, 20 °C): 2.68 μ_{B} . Mass spectrum, LSIMS (CsI calibration): simulated (relative intensity), 1262.5 (1.00), 1263.5 (0.97), 1264.5 (0.95), 1261.5 (0.95), 1260.5 (0.85), 1265.5 (0.72), 1266.5 (0.65), 1259.5 (0.60); found (relative intensity), 1262.0 (1.00), 1263.0 (0.96), 1264.0 (0.90), 1261.0 (0.85), 1260.0 (0.80), 1259.0 (0.70), 1265.0 (0.65), 1266.0 (0.55).

Preparation of [(OEP)WOs(OEP)] (2). Vacuum pyrolysis of a mixture of W(OEP)(PEt₃)₂ (25.3 mg) and Os(OEP)(py)₂ (15.1 mg) at 6×10^{-6} Torr and 210 °C (8 h) yields 29.1 mg of a mixture of 20% [W(OEP)]₂, 42% [(OEP)WOs(OEP)], and 38% [Os(OEP)]₂. Isolation of the mixed species is effected by redox titration exactly as prescribed above in the preparation of **1**. The yield of [(OEP)WOs(OEP)] is 4.6 mg, 37.7%.

UV-vis [nm (C₆H₆, log ϵ): Soret Os(OEP) 352 (4.49), Soret W(OEP) 389 (4.57). ^1H NMR (ppm, C₆D₆): δ -82.50 (s, 4H, W H_{meso}); -27.05 (s, 4H, Os H_{meso}); 22.40 (m, 8H, W-CH₂CH₃), 19.50 (m, 8H, W-CH₂CH₃); 8.05 (m, 8H, Os-CH₂CH₃), 7.20 (m, 8H, Os-CH₂CH₃); -0.45 (t, 24H, W-CH₂CH₃); 1.60 (t, 24H, Os-CH₂CH₃). μ_{eff} (Evans method, toluene, 20 °C): 2.62 μ_{B} . Mass spectrum, LSIMS (CsI calibration): simulated (relative intensity), 1440.6 (1.00), 1438.6 (0.94), 1439.6 (0.90), 1437.6 (0.62), 1441.6 (0.60), 1436.6 (0.55), 1442.6 (0.53); found (relative intensity), 1440.3 (1.00), 1438.3 (0.96), 1439.3 (0.90), 1437.3 (0.60), 1436.3 (0.62), 1441.3 (0.58), 1442.3 (0.49).

Preparation of [(OEP)MoRu(TPP)] (3). Vacuum pyrolysis of a mixture of Mo(OEP)(PhC \equiv CPh) (35 mg) and Ru(TPP)(py)₂ (25 mg) at 6×10^{-6} Torr and 210 °C (4 h) yields 32 mg of a mixture of 14% [Mo(OEP)]₂, 78% [(OEP)MoRu(TPP)], and 8% [Ru(TPP)]₂. Isolation of the mixed species is effected by redox titration exactly as prescribed above in the preparation of **1**. The yield of [(OEP)MoRu(TPP)] is 13.9 mg, 43.7%.

UV-vis [nm (C₆H₆, log ϵ): Soret Ru(TPP) 375 (4.56), Soret Mo(OEP) 396 (4.78). ^1H NMR (ppm, C₆D₆): δ -9.7 (s, 4H, Mo H_{meso}); 1.28 (s, 8H, Ru H_B); 8.23 (m, 8H, Mo-CH₂CH₃), 6.80 (m, 8H, Mo-CH₂CH₃); 6.90 (d, 4H, Ru endo *o*-phenyl), 7.79 (t, 4H, Ru endo *m*-phenyl); 5.89 (d, 4H, Ru exo *o*-phenyl), 6.78 (t, 4H, Ru exo *m*-phenyl); 7.49 (t, 4H, Ru *p*-phenyl); 1.09 (t, 24H, Mo-CH₂CH₃). μ_{eff} (Evans method, toluene, 20 °C): 2.71 μ_{B} . Mass spectrum, LSIMS (CsI calibration): simulated (relative intensity), 1342.4 (1.00), 1343.4 (0.99), 1344.4 (0.99), 1341.4 (0.93), 1340.4 (0.78), 1345.4 (0.71), 1339.4 (0.59); found (relative intensity), 1342.1 (1.00), 1343.1 (0.99), 1344.1 (0.98), 1341.1 (0.92), 1340.1 (0.79), 1345.1 (0.76), 1339.1 (0.59).

Results

^1H NMR. The ^1H NMR of [(OEP)MoRu(OEP)] (**1**) is shown in Figure 1. The corresponding spectrum of [(OEP)WOs(OEP)] (**2**) is qualitatively identical to that of [(OEP)MoRu(OEP)] as seen in Table 1. In each case two distinct sets of ethyl protons are manifest, with one significantly shifted from the diamagnetic position observed for isoelectronic [Re(OEP)]₂. Two sets of meso protons are also observed, and both exhibit large upfield isotropic shifts from the H_{meso} resonance in [Re(OEP)]₂.

(11) Selwood, P. W. *Magnetochemistry*; Interscience: New York, 1956.

(12) Evans, D. F. *J. Chem. Soc.* **1959**, 2003–2005.

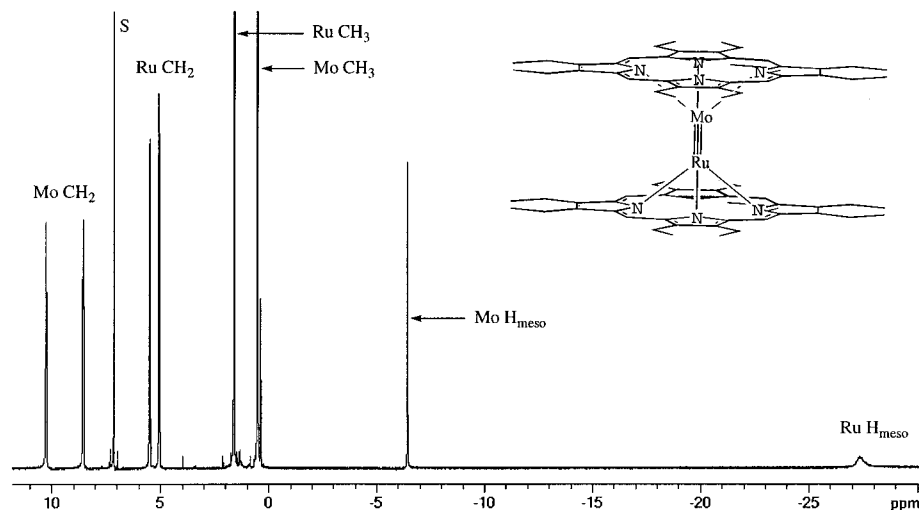


Figure 1. 500 MHz (C_6D_6) 1H NMR of [(OEP)MoRu(OEP)] (**1**) at 20 °C. The spectrum of [(OEP)WOs(OEP)] is qualitatively identical; chemical shifts are shown in Table 1.

Table 1. 1H NMR^a and Magnetic Susceptibility^b of d^{10} Metal–Metal-Bonded Porphyrin Dimers

dimer	μ_{eff} (μ_B)	$\delta(H_{\text{meso}})$ (s)	$\delta(-CH_2)$ (q)	$\delta(-CH_3)$ (t)
[Re(OEP)] ₂	$\leq 0.8^c$	6.45 (s)	3.73, 3.98	1.65
[(OEP)MoRu(OEP)]	2.68	−8.10 (Mo) −30.90 (Ru)	5.20, 5.70 (Ru) 9.10, 10.98 (Mo)	1.75 (Ru) 0.55 (Mo)
[(OEP)WOs(OEP)]	2.62	−27.1 (W) −82.50 (Os)	8.05, 7.20 (Os) 19.50, 22.40 (W)	1.60 (Os) −0.45 (W)

^a All spectra taken in toluene- d_8 . ^b Evans method in toluene- d_8 at 20 °C. ^c No effect observed.

Assignments have been made on the basis of 2D COSY spectra and comparison with OEP–TPP analogues.

The large isotropic shifts exhibited in the 1H NMR spectra of the heterometallic dimers indicate the existence of paramagnetism in these molecules. We have used the method developed by Evans¹² to measure solution magnetic susceptibilities with NMR spectroscopy, and these measurements are consistent with the presence of two unpaired electrons at room temperature ($\mu_{\text{eff}} = 2.62 \mu_B$). However, the traditional Cotton molecular orbital diagram for metal–metal bonds predicts a diamagnetic ground state $\sigma^2\pi^4\delta^2\delta^*2$ configuration for the 10 d-electron system. Indeed, the 10-electron [Re(OEP)]₂ metalloporphyrin homodimer exhibits no paramagnetic susceptibility by the Evans method nor displays any isotropic shifts in the 1H NMR.

An energy difference between the δ^* and π^* orbitals which is far less than the thermal energy available at room temperature could result in significant population of the first excited electronic state, $\sigma^2\pi^4\delta^2\delta^*\pi^*2$, and explain the room-temperature contact-shifted 1H NMR resonances and solution magnetic susceptibility data. However, variable-temperature 1H NMR studies of **1–3** indicate the population of a single spin state throughout the limited temperature range examined (−90 to +90 °C). There is no qualitative difference in magnetic behavior between the [(OEP)MoRu(OEP)] dimer (**1**) and the [(OEP)MoRu(TPP)] dimer (**3**). As shown in Figure 2, the chemical shift positions vary linearly with inverse temperature, consistent with the presence of a paramagnetic ground electronic configuration. Such behavior implies that temperature-dependent thermal population of an excited state is not in effect.

Solid-State SQUID Magnetic Susceptibility. Variable-temperature (2–300 K) solid-state magnetic susceptibility of [(OEP)MoRu(OEP)] was also measured in order to determine if the paramagnetic state is the ground electronic configuration. Plots of χ vs T and μ_{eff} vs T (Figure 3) indicate that the magnetic moment of the dimer is $0.44 \mu_B$ at 2 K and tends toward the

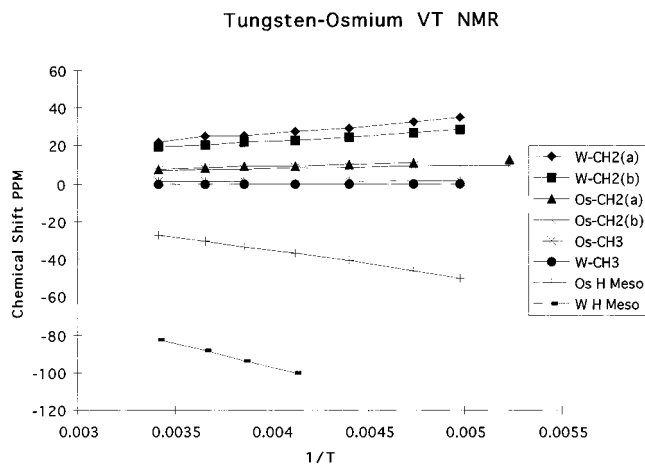


Figure 2. Variable-temperature 1H NMR of [(OEP)WOs(OEP)] (**2**) in $C_6D_5CD_3$: observed chemical shift as a function of inverse temperature.

spin-only value expected for an $S = 1$ spin state ($2.83 \mu_B$) as the temperature is raised. The data are strikingly similar to those we recently reported for 12-electron Ru_2 and Os_2 porphyrin homodimers.¹³ Curve-fitting analysis using the well-established zero-field splitting (ZFS) model¹⁴ provided reasonable values for the varied parameters ($D \approx 600\text{--}800 \text{ cm}^{-1}$, $g_{\parallel} = 1.8$, $g_{\perp} = 2.2$, fraction of impurity = 1.9%, g of impurity = 2.1, TIP =

(13) Godwin, H. A.; Collman, J. P.; Marchon, J.-C.; Maldivi, P.; Yee, G. T.; Conklin, B. J. *Inorg. Chem.* **1997**, *36*, 3499–3502.

(14) (a) Carlin, R. L. *Magnetochemistry*; Springer-Verlag: Berlin, 1986. (b) Cotton, F. A.; Pedersen, E. *Inorg. Chem.* **1975**, *14*, 388–391. (c) Telsler, J.; Drago, R. S. *Inorg. Chem.* **1984**, *23*, 3114–3120. (d) Cotton, F. A.; Ren, T.; Eglin, J. L. *J. Am. Chem. Soc.* **1990**, *112*, 3439–3445. (e) Bonnet, L.; Cukiernik, F. D.; Maldivi, P.; Giroud-Godquin, A.-M.; Marchon, J.-C.; Ibn-Elhaj, M.; Guillon, D.; Skoulios, A. *Chem. Mater.* **1994**, *6*, 31–38. (f) Cukiernik, F. D.; Maldivi, P.; Marchon, J.-C. *Inorg. Chim. Acta* **1994**, *215*, 203–207.

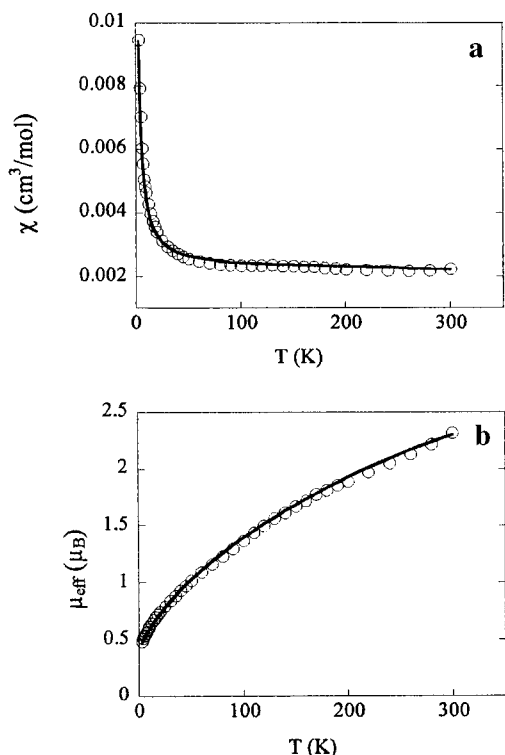


Figure 3. Data points and adjusted curves for the magnetic susceptibility (a) and the magnetic moment (b) of [(OEP)MoRu(OEP)]. The fits were obtained with a value of $D = 800 \text{ cm}^{-1}$ and the following values of the adjusted parameters: $g_{\parallel} = 1.8$; $g_{\perp} = 2.2$; $TIP = 4 \times 10^{-5}$; fraction of paramagnetic impurity = 1.9%; g of impurity = 2.1.

4×10^{-5}). Estimates of the ZFS parameter, D , are in close agreement with those obtained for related molecules¹³ and may be understood as a consequence of large second-order spin-orbit coupling and axial distortion of the crystal field from cubic symmetry due to the presence of a multiple metal-metal bond. Although the $S = 1$ d^{10} species was found to be ESR silent, we were able to obtain an ESR spectrum of the $S = 1/2$, d^9 dimer, [(OEP)MoRu(OEP)]PF₆. The experimental g values, $g_{\parallel} = 1.973$ and $g_{\perp} = 1.952$ (see Supporting Information), are in qualitative agreement with those determined by the fit for **1**. Thus, the overall magnetic behavior is consistent with large zero-field splitting of a triplet ground state.¹⁵

X-ray Crystallography. Structural characterization of heterometallic metalloporphyrin dimers demands preparation of a dimer with distinct porphyrins for each metal. An X-ray diffraction study of [(OEP)MoRu(OEP)] or [(OEP)WOs(OEP)] would likely be plagued by statistical disorder and averaging of the two metalloporphyrin congeners. To avoid such issues, we prepared and structurally characterized a molybdenum-ruthenium metal-metal-bonded dimer using one octaethylporphyrin (OEP) and one tetraphenylporphyrin (TPP) ligand. Despite considerable effort to obtain single crystals of neutral

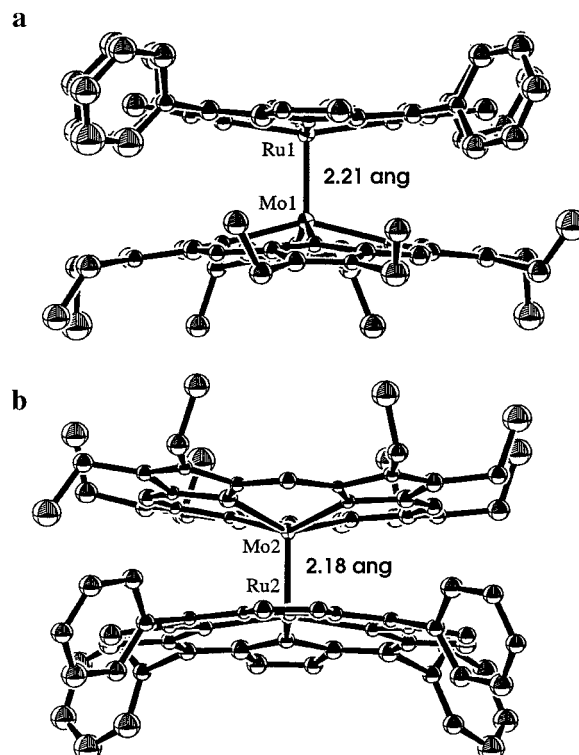


Figure 4. ORTEP plot of [(OEP)MoRu(TPP)]PF₆ illustrating the two separate dimers in the asymmetric unit: (a) Mo1-Ru1 (ligands eclipsed), 2.211(2) Å; (b) Mo2-Ru2 (staggered), 2.181(2) Å.

[(OEP)MoRu(TPP)] and [(OEP)WOs(TPP)], we were unable to do so.¹⁶ However, oxidizing the dimers to a cation offered the opportunity to experiment with various counteranions and apparently favored the crystallinity of the resulting solid. After several months of experimentation we obtained X-ray-quality crystals of [(OEP)MoRu(TPP)]PF₆ (**3**⁺). Suitable crystals of [(OEP)WOs(TPP)]PF₆ have not yet been obtained, and continued attempts have been hampered by the extreme sensitivity of WOs dimers toward oxidation and metal-metal bond cleavage.

Crystals of **3**⁺ formed in the space group $P2_1/n$ with eight dimers in the unit cell. The asymmetric unit was found to contain structural isomers, **3a**⁺ and **3b**⁺ (Figure 4), most likely as a result of a steric preference for the staggered conformation and an electronic stabilization in the eclipsed conformation (vide infra). That both isomers are simultaneously exhibited in the asymmetric unit implies that the steric and electronic forces are very similar in magnitude.¹⁷ Figure 5 gives top-down views of the molecules, and selected structural parameters are summarized in Table 2. Each isomer contains a MoRu⁵⁺ unit, but the metal-metal bond lengths are slightly different. The eclipsed isomer, **3a**⁺, exhibits a metal-metal separation of 2.211(2) Å, while the staggered isomer, **3b**⁺, exhibits a slightly shorter bond of 2.181(2) Å. Furthermore, the Ru atom is displaced from the N₄ (TPP) plane by 0.334 Å in the eclipsed isomer but by only 0.295 Å in the staggered one. The longer Mo-Ru bond and larger Ru-N₄ displacement in the eclipsed isomer are most likely to be consequences of the steric strain incurred upon rotation of the porphyrin ligands to the eclipsed conformation.

(15) There also exists the possibility of a magnetically equivalent $\sigma^2\pi^4\delta^2\delta^*\pi^*$ (³E) ground state, arising as a result of accidental degeneracy of the δ^* and π^* orbitals. Such a situation has been observed for Os₂⁶⁺ dimers; see: (a) Miskowski, V. M.; Gray, H. B. *Top. Curr. Chem.* **1997**, *191*, 41–57. (b) Cotton, F. A.; Ren, T.; Eglin, J. L. *Inorg. Chem.* **1991**, *30*, 2552–2558. However, low-temperature magnetic susceptibility data for molecules with the $\sigma^2\pi^4\delta^2\delta^*\pi^*$ ground electronic configuration are not accurately described by the ³A₂-ZFS model. That the magnetic data presented herein are perfectly described by the ZFS model is necessary and sufficient evidence to support a π^{σ^2} , ³A₂ ground electronic configuration for d⁴–d⁶ (porphyrin)MoRu(porphyrin) metal-metal-bonded species (see: Cotton, F. A.; Ren, T.; Wagner, M. J. *Inorg. Chem.* **1993**, *32*, 967, column 2, paragraph 2).

(16) Our inability to obtain X-ray-quality crystals of neutral metalloporphyrin dimers is likely a consequence of their poor but partial solubility in nearly all solvents. Gentle lowering of temperature afforded microcrystalline material only.

(17) Bray, K. L.; Drickamer, H. G.; Mings, M. P.; Watson, M. J.; Shapley, J. R. *Inorg. Chem.* **1991**, *30*, 864–866.

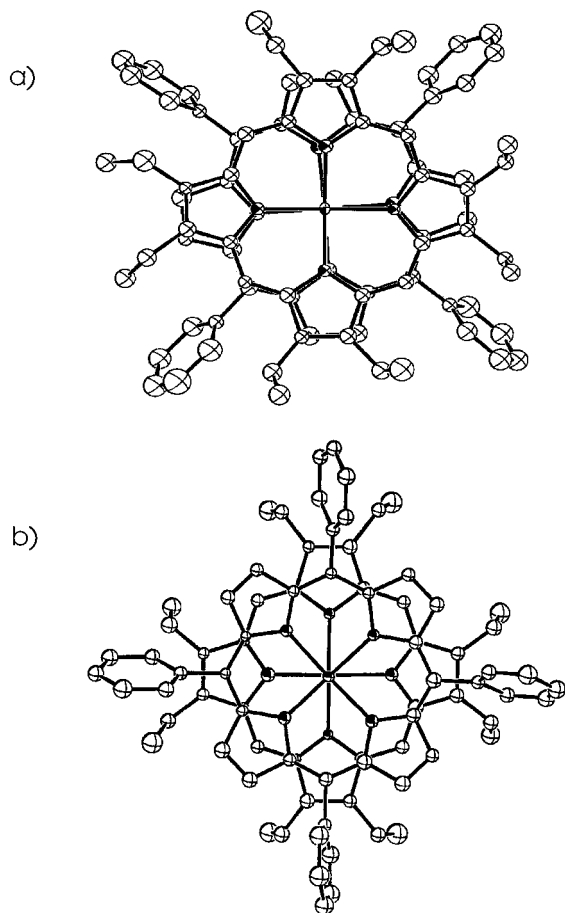


Figure 5. (a) ORTEP plot of $3a^+$ as viewed down the Mo1–Ru1 bond axis: porphyrin cores are rotated 4.4° ; $N_4-N'_4 = 3.106(4)$ Å; Mo1– $N_4 = 0.562(2)$ Å; Ru1– $N'_4 = 0.334(2)$ Å. (b) ORTEP plot of $3b^+$ as viewed down the Mo2–Ru2 bond axis: porphyrin cores are rotated 43.5° ; $N_4-N'_4 = 3.054(4)$ Å; Mo2– $N_4 = 0.578(2)$ Å; Ru2– $N'_4 = 0.295(2)$ Å.

Vibrational Spectroscopy. The metal–metal bonds contained in **1**, **2**, and 3^+ , as well as the Re_2^{4+} unit in $[Re(OEP)]_2$, have been characterized by resonance Raman (RR) spectroscopy (Figures 6 and 7). In each case enhancement of a mode assigned as the metal–metal stretch was effected with UV excitation (363.8 nm) into the blue side of either the Ru, Os, or Re metalloporphyrin Soret band (see Figure 8). Assignment of the ν_{MM} modes (Table 3) was made on the basis of similar vibrational studies of other multiply bonded metal–metal dimers,² depolarization ratios, subtraction of the spectra obtained from the corresponding metalloporphyrin monomers, and comparison with existing normal coordinate analyses of metal–metal-bonded porphyrin dimers¹⁸ and Ni(OEP)¹⁹ and Cu(TPP)²⁰ monomers. Metal–metal bond force constants of 2.97 mdyne/Å (**1**), 3.93 mdyne/Å (**2**), and 4.18 mdyne/Å ($[Re(OEP)]_2$) have been estimated with the diatomic oscillator approximation²¹ and are consistent with numerous existing data indicating that 5d–5d metal–metal bonds are typically 20–30% stronger than cor-

responding 4d–4d metal–metal bonds.²² In addition to the “predominantly” metal–metal stretches, a second intense low-frequency band, ν_8 , is also observed at approximately 350 cm^{-1} in the RR spectra of each dimer. This band has been assigned according to the scheme developed by Kitagawa and corresponds to an in-plane porphyrin breathing mode of the metal–OEP species.¹⁹

Discussion

Ground Electronic Configuration of (MoRu)⁴⁺ and (WOs)⁴⁺ Dimers. Large isotropic shifts in the 1H NMR of $[(OEP)MoRu(OEP)]$, $[(OEP)MoRu(TPP)]$, and $[(OEP)WOs(OEP)]$ were the first clues suggesting that these d^{10} intertriad heterodimers did not exhibit the $\sigma^2\pi^4\delta^2\pi^{*2}$ molecular orbital diagram which has been shown to be consistent with the spectroscopic properties of homologous $Re^{II}-Re^{II}$,⁹ $Ru^{III}-Ru^{III}$,²³ and $Os^{III}-Os^{III}$ ²³ porphyrin dimers. We confirmed a paramagnetic ground state for the MoRu and WOs complexes through the use of variable-temperature NMR (**1–3**) and solid-state SQUID magnetometry (**1**). This observation is consistent with either of two perturbations ($\sigma^2\pi^4\delta^2\pi^{*2}$ and $\sigma^2\pi^4\delta^{nb2}\pi^{*2}$) on the traditional molecular orbital description for metal–metal bonding. Stabilization of the π^* orbitals below the level of $\delta^{(*/nb)}$ has been observed previously^{2,5} but only in a few Ru_2^{6+} and Os_2^{6+} complexes with extremely π -basic ligand sets other than porphyrins.

δ Bonding in (MoRu)⁴⁺ and (WOs)⁴⁺ Dimers. Existence of a δ bond (δ vs δ^{nb} in the MO descriptions above) in intertriad metalloporphyrin dimers could not be tacitly assumed since the porphyrins do not require an eclipsed or nearly eclipsed conformation as is the case with most other (bridging) ligands. Since the face-to-face nature of δ overlap makes inefficient use of d_{xy} radial distribution maxima, severe energetic mismatch of the atomic d_{xy} orbitals from metals of different triads may very well preclude δ -bond formation altogether. For example, variable-temperature NMR analyses of the rotational barriers about MoW, Mo₂, and W₂ porphyrin dimers has shown the MoW δ bond to be the weakest.^{18,24}

We first attempted to discover evidence of δ bonding in MoRu and WOs porphyrin dimers through complete band shape analysis of dynamic NMR spectra. However, VT NMR investigations of $[(OEP)MoRu(OEP)]$ and $[(OEP)WOs(OEP)]$ (TOEP = monotoyloctaethylporphyrin) proved inconclusive and could only establish an upper limit of 8 kcal/mol for any δ bonds that may be present in the ground electronic configurations of these molecules.¹ Since δ overlap is maximized in an eclipsed conformation and nonexistent in a staggered conformation, structural characterization of a MoRu or WOs dimer was then viewed as the ideal spectroscopic method for identification of δ overlap.

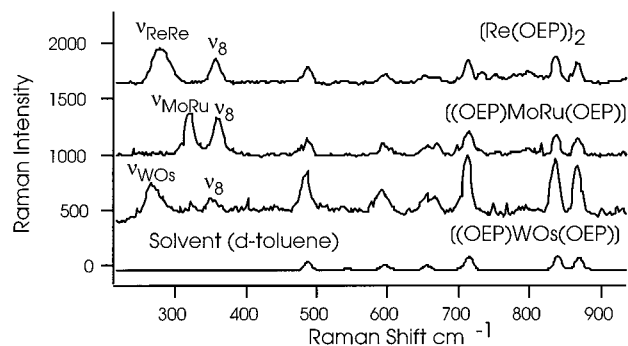
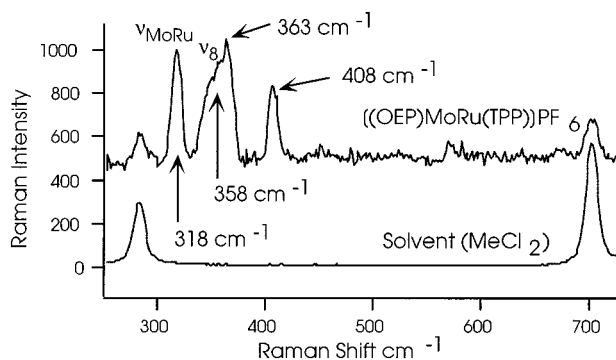
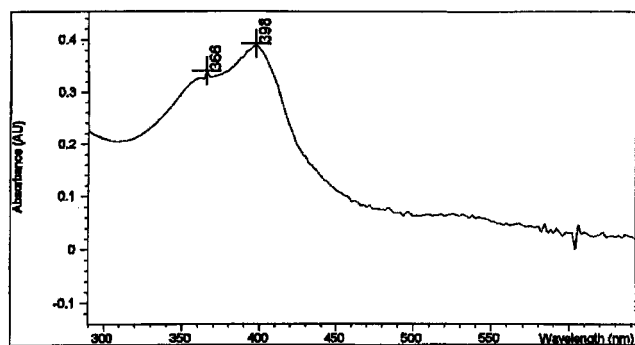
In an attempt to avoid intermediate, ambiguous porphyrin–porphyrin twist angles,²⁵ we prepared octaethylporphyrin/

- (18) Collman, J. P.; Harford, S. T.; Franzen, S. F.; Eberspacher, T. A.; Shoemaker, R.; Woodruff, W. H. *J. Am. Chem. Soc.* **1998**, *120*, 1456–1465.
- (19) (a) Kitagawa, T.; Abe, M.; Ogoshi, H. *J. Chem. Phys.* **1978**, *69*, 4516–4525. (b) Abe, M.; Kitagawa, T.; Kyogoku, Y. *J. Chem. Phys.* **1978**, *69*, 4526–4534.
- (20) Atamian, M.; Donohoe, R. J.; Lindsey, J. S.; Bocian, D. F. *J. Phys. Chem.* **1989**, *93*, 2236–2243.
- (21) $k = (3.55 \times 10^{17})\mu\nu^2$, where k = force constant (mdyne/Å), μ = reduced mass of the two metal atoms (g), and ν = vibrational frequency (cm^{-1}).

- (22) Manning, M. C.; Trogler, W. C. *J. Am. Chem. Soc.* **1983**, *105*, 5311–5320.
- (23) (a) Asahina, H.; Zisk, M. B.; Hedman, B.; McDevitt, J. T.; Collman, J. P.; Hodgson, K. O. *J. Chem. Soc., Chem. Commun.* **1989**, 1360–1362. (b) Tait, C. D.; Garner, J. M.; Collman, J. P.; Sattelberger, A. P.; Woodruff, W. H. *J. Am. Chem. Soc.* **1989**, *111*, 7806–7811. (c) Collman, J. P.; Prodollet, J. W.; Leidner, C. R. *J. Am. Chem. Soc.* **1986**, *108*, 2916.
- (24) (a) Collman, J. P.; Garner, J. M.; Hembre, R. T.; Ha, Y. *J. Am. Chem. Soc.* **1992**, *114*, 1292.
- (25) (a) Collman, J. P.; Barnes, C. E.; Swepston, P. N.; Ibers, J. A. *J. Am. Chem. Soc.* **1984**, *106*, 3500–3510. (b) Yang, C.-H.; Dzuga, S.; Goedken, V. L. *J. Chem. Soc., Chem. Commun.* **1986**, 1313–1315. In these metal–metal-bonded OEP–OEP and TPP–TPP dimers, porphyrin–porphyrin twist angles of 22.5° and 18° are observed.

Table 2. Selected Structural Parameters (Å) for [(OEP)MoRu(TPP)]PF₆ (3⁺)

	Mo–Ru	Mo–N ₄	Ru–N' ₄	N ₄ –N' ₄	N–Mo–Ru–N' dihedral angle ^a	MO diagram (bond order)
3a ⁺	2.211(2)	0.562	0.334	3.11	4.5	$\sigma^2\pi^4\delta^2\pi^{*1}$ (3.5)
3b ⁺	2.181(2)	0.578	0.295	3.05	43.4	$\sigma^2\pi^4\delta^{nb2}\pi^{*1}$ (2.5)

^a Geometric mean given in deg.**Figure 6.** Low-frequency RR spectra upon excitation at 363.8 nm for **1**, **2**, and [Re(OEP)]₂. Samples were prepared in toluene-*d*₈ solution and flame sealed. Solvent resonances were not subtracted from the raw data but are given for comparison. All spectra are baseline corrected. Sample stability was confirmed by ¹H NMR analysis following excitation.**Figure 7.** Low-frequency RR spectra upon excitation at 363.8 nm for **3**⁺. Assignment of the bands at 358 and 363 cm⁻¹ to OEP-based breathing modes was made according to the descriptions of ν_8 and ν_{35} in ref 20a (see p 4524). An analogous mode for TPP core-breathing is expected near 410 cm⁻¹ (ref 19), and the observed band at 409 cm⁻¹ has been thus assigned.**Figure 8.** Electronic absorption spectrum for **1** in benzene. Separate Soret bands for the Mo(OEP) and Ru(OEP) species are observed at 398 and 366 nm, respectively. The corresponding bands are observed at 389 and 352 nm for [(OEP)WOs(OEP)]. Other than the Soret bands, the spectra are essentially featureless.

tetraphenylporphyrin analogues of **1** and **2**. With this combination, an eclipsed conformation requires only phenyl proton interactions between the corresponding *meso*-positions, while intermediate porphyrin–porphyrin twist angles (15–30°) would

eclipse the *meso*-phenyl positions with H_B-ethyl substituents. A perfectly staggered conformation is still expected to be the steric energy minimum, however, since the eight interior nitrogen atoms should dominate contributions to the overall steric repulsion.

δ Bonding in (MoRu)⁵⁺ and the Bond Paradox. Structural characterization of **3**⁺ indicates that, indeed, a δ bond may exist in the ground electronic description for [(OEP)MoRu(TPP)]PF₆. However, the δ -bond strength is apparently very close in absolute energy to the excess steric strain incurred upon rotation from the staggered conformation to the eclipsed. The bulk of this strain is most likely N–N' repulsion, and to a lesser extent H–H repulsion along the periphery of the dimer may also contribute. We have estimated this energy through MM2 steric computations using a recent version of Chem 3D.²⁶ Atomic coordinates from the staggered isomer, **3b**⁺, were fed into the program and steric computations performed as a function of N–Mo–Ru–N' dihedral angle. The metal–metal vector and porphyrin–porphyrin separation were held fixed, and a value of 5.5 kcal/mol was obtained upon rotation to the eclipsed conformation. In the actual crystals, this excess strain is (at least partially) relieved by increase of the porphyrin–porphyrin separation (see Table 2).

Because the crystals were grown at ambient temperature, we may only conclude that the two molecular orbital descriptions— $\sigma^2\pi^4\delta^2\pi^{*1}$ and $\sigma^2\pi^4\delta^{nb2}\pi^{*1}$ —are within 200 cm⁻¹ of each other in absolute energies. We are pursuing low-temperature recrystallization of **3**⁺ in an attempt to trap the molecules in one or the other conformation, but thus far our efforts have been unsuccessful.

That one or the other of the two metal–metal bonds exhibited in Figure 4 is stronger poses an interesting question. The eclipsed dimer demonstrates a Mo–Ru bond length of 2.211(2) Å and molecular orbital diagram $\sigma^2\pi^4\delta^2\pi^{*1}$ (BO = 3.5). Interestingly, the metal–metal bond exhibited by the staggered dimer is shorter, 2.181(2) Å, despite the lack of a δ bond (BO = 2.5)! The resolution of this apparent paradox comes with simple considerations of steric and electronic energetics. The eclipsed dimer exchanges the formation of a δ bond for loss of σ and π overlap: increase of the metal–metal bond length and porphyrin–porphyrin separation may be expected to relieve the excess steric energy, but interaction energies of Mo and Ru d_z^2 , d_{xz} , and d_{yz} orbitals are also decreased by placing them farther apart in space. The staggered dimer contains stronger σ and π bonds but has no δ bond; the eclipsed dimer contains a δ bond along with a weaker set of σ and π bonds.

Use of Resonance Raman Spectral Contributions. Resonance Raman spectroscopy has often been used to characterize metal–metal bond vibrations by identification of their stretching frequencies and calculation of the corresponding stretching force constants.² A single, sharp metal–metal stretching band in the solution resonance Raman spectrum of **3**⁺ (Figure 7) allows us to reach a very important conclusion—the presence or absence

(26) Version 3.5 (July 1996) from Cambridge Soft Corp., Cambridge, MA 02139. The outputs for through-space nonbonded interactions were calculated using an MM2 force field derived from Allinger's MM2 program (QCPE 395) and Ponder's TINKER system (unpublished).

Table 3. Vibrational Data for d¹⁰ and d¹² Metal–Metal-Bonded Porphyrin Dimers

dimer	ν_{MM} (cm ⁻¹)	k (mdyn/Å)	bond order	MO diagram	ref
[Ru ^{II} (OEP)] ₂	285	2.42	2.0	$\sigma^2\pi^4\delta^2\delta^{*2}\pi^{*2}$	23b
[Ru ^{III} (OEP)] ₂ (PF ₆) ₂	310	2.70	3.0	$\sigma^2\pi^4\delta^2\delta^{*2}$	23b
[(OEP)MoRu(OEP)]	320	2.97	3.0/2.0	$\sigma^2\pi^4\delta^{(nb)2}\pi^{*2}$	a
[(OEP)MoRu(TPP)]PF ₆	318	2.93	3.5/2.5	$\sigma^2\pi^4\delta^{(nb)2}\pi^{*1}$	a
[Os ^{II} (OEP)] ₂	233	3.04	2.0	$\sigma^2\pi^4\delta^2\delta^{*2}\pi^{*2}$	31
[(OEP)WOs(OEP)]	267	3.93	3.0/2.0	$\sigma^2\pi^4\delta^{(nb)2}\pi^{*2}$	a
[Os ^{III} (OEP)] ₂	266	3.96	3.0	$\sigma^2\pi^4\delta^2\delta^{*2}$	31
[Re ^{II} (OEP)] ₂	276	4.18	3.0	$\sigma^2\pi^4\delta^2\delta^{*2}$	a

^a This work.

of a δ bond has no clear implication on the force constant for the metal–metal stretch. This conclusion may be understood as a result of the weak nature of the δ bond relative to the σ and π , as well as an incursion of longer metal–metal separations through increased steric repulsions associated with the eclipsed conformation. In the case of neutral [(OEP)MoRu(OEP)], if the eclipsed and staggered conformations persist and exhibit metal–metal bonds of significantly different strengths, distinct metal–metal stretches should be seen in the RR spectrum. However, the solution RR spectrum of **1** (Figure 6) also demonstrates a single, well-shaped band confidently assigned as ν_{MoRu} . Apparently the two metal–metal bonds of the (hypothetical) conformations have comparable strengths, despite being of different order and different length.

Comparison of the MoRu⁴⁺ metal–metal vibration in Figure 6 with the corresponding MoRu⁵⁺ stretch in Figure 7 illustrates an important point concerning the validity of vibrational spectroscopy for metal–metal bond characterization. Our recent simple normal coordinate analysis¹⁸ of metal–metal-bonded porphyrin dimers demonstrated that the observed ν_{MM} is predominantly, but not entirely, diatomic in nature. Our results are consistent with previous²⁷ analyses suggesting that observed metal–metal stretches are purest for metal–metal bonds containing heavy metals.²⁸ Since the MoRu bonds are composed of two 4d metals, the potential energy distributions (PED) of the observed ν_{MM} modes are predicted to contain 80% ν_{MM} character and, thus, 20% character from displacement of ligand internal coordinates. For metal–metal bonds with one third-row metal, the observed mode is calculated to contain approximately 90% ν_{MM} character, and metal–metal bonds between two third-row metals are predicted to exhibit metal–metal stretching modes which are 95% devoid of ligand-based contributions to the observed PED. Thus, the observed ν_{MoRu} stretches are expected to be particularly sensitive to the ligand identity, and conclusions drawn from comparison of a ν_{MoRu} stretch in [(OEP)MoRu(OEP)] with a ν_{MoRu} stretch from [(OEP)MoRu(TPP)]PF₆ are not likely to be strictly reflective of differences in metal–metal bond strengths. In the present case, we would fully expect the MoRu⁵⁺ to be stronger than the MoRu⁴⁺, but the stretching frequencies and corresponding force constants imply otherwise.²⁹ The normal mode coordinate analysis is consistent with a lowering of the observed ν_{MoRu} stretch on the order of 5 cm⁻¹ upon substitution of a TPP (MW = 624 g/mol) for an OEP (MW = 532 g/mol) ligand due to the difference in reduced mass. In light of this correction, the resonance Raman data are consistent with removal of a metal–metal antibonding electron upon oxidation of MoRu⁴⁺.³⁰

In the case of [(OEP)WOs(OEP)], magnetic and ¹H NMR data are qualitatively identical to those for [(OEP)MoRu(OEP)] and indicate the presence of two unpaired electrons in a degenerate HOMO. However, we have thus far been unable to provide any direct evidence for a δ bond between W and Os. The resonance Raman metal–metal stretch exhibits a force constant, 3.93 mdyn/Å, which is slightly less than those found for isoelectronic [Os^{III}(OEP)]₂(PF₆)₂³¹ and [Re^{II}(OEP)]₂ porphyrin homodimers, both of which are known to contain diamagnetic $\sigma\pi\pi$ triple bonds ($\sigma^2\pi^4\delta^2\delta^{*2}$, Table 3).³² That the Os^{III}–Os^{III} force constant is somewhat smaller than that observed for Re^{II}₂ is likely a consequence of the higher oxidation state and constricted orbitals of Os^{III} centers. Inspection of the force constants in Table 3 implies that [(OEP)WOs(OEP)] contains a weak triple bond ($\sigma\pi\delta$ as opposed to $\sigma\pi\pi$ is expected to be weaker), however; since the MoRu⁵⁺ data does not distinguish between molecules with or without δ bonds (the X-ray structure indicates that an equilibrium between the two conformations should exist in solution),³³ this crude conclusion is called into serious question. Indeed, we feel it is most likely that the increased WOs metal–metal separation in addition to the severe d_{xy} energetic mismatch will greatly reduce or even preclude W–Os δ -bond formation altogether, and thus, the bonding in **2** may most likely be described as a strong $\sigma\pi$ double bond.³⁴

- (30) For several years we have been attempting to gather thermochemical data for correlation with the vibrational spectra of metal–metal bonds, but as yet, the experimental difficulties and assumptions inherent in thermochemical studies of such species have precluded any success.
- (31) Tait, C. D.; Garner, J. M.; Collman, J. P.; Sattelberger, A. P.; Woodruff, W. H. *J. Am. Chem. Soc.* **1989**, *111*, 9072–9077.
- (32) The resonance Raman spectrum of the [Re(OEP)]₂ sample was rerun after 18 months for use as a standard for comparison with other spectra. We were surprised to find the later spectrum exhibited distinct peaks at 267 and 288 cm⁻¹ (available as Supporting Information) as opposed to the single band initially observed at 275 cm⁻¹. The aged sample did contain a solid precipitate which was not originally present, and we feel the later spectrum was of the solid precipitate (solvent peaks were not observed). We have no explanation for why there might be two metal–metal stretching peaks in the solid, but since their average (278 cm⁻¹) is within experimental error of the solution band, our calculated force constant is accurate for either data set. Unfortunately, we have been unsuccessful in obtaining analogous solid-state RR data from crystals of **3**⁺.
- (33) The proposition of an equilibrium between eclipsed and staggered isomers in solution might be proven by EXAFS data demonstrating two separate Mo–Ru bond lengths, but we have not yet had the opportunity to try the experiment (furthermore, the low resolution of EXAFS, typically 0.03–0.05 Å, calls the experiment into question).
- (34) Our structural characterization of MoOs and WRu dimers (immediately following manuscript) demonstrates a tendency toward staggered conformations (weak, if any, δ bonding) with longer metal–metal bonds. Interestingly, the WOs⁴⁺ force constant, 3.93 mdyn/Å, is still considerably larger than that for the analogous Os₂⁴⁺ $\sigma\pi$ double bond (3.04 mdyn/Å). In general, our preliminary resonance Raman and X-ray data suggest that heterometallic bonds are 15–25% stronger than corresponding homometallic bonds of the same order and composition. The immediately following manuscript provides further insight into these data.

(27) Quicksall, C. O.; Spiro, T. G. *Inorg. Chem.* **1969**, *8*, 2363–2367.

(28) A variety of consequences lead to this conclusion; for in-depth discussions, the reader is referred to refs 18 and 27.

(29) We would have preferred to avoid this situation altogether, but the X-ray crystallography demands a mixed-porphyrin species, while our vast collection of existing vibrational spectra all contain metal–metal bonds with the same porphyrins (OEP).

Conclusions

The first magnetic susceptibility, NMR, resonance Raman, and X-ray crystallographic studies of intertriad heterodimers [(OEP)MoRu(OEP)] (**1**), [(OEP)W(OEP)] (**2**), and [(OEP)MoRu(TPP)]PF₆ (**3**⁺) have been used to demonstrate an unusual molecular orbital diagram, $\sigma^2\pi^4\delta^{(nb)2}\pi^{*1}$ or 2 , which has never been observed before in metal–metal bonded metalloporphyrin dimers. The paramagnetism of the neutral dimers **1–3** is manifest in the large isotropic shifts observed in the ¹H NMR of these molecules, and an *S* = 1 spin state has been demonstrated by Evans method and SQUID magnetic susceptibility measurements. The presence of a δ bond in **3**⁺ is implied by the unprecedented observation that both the eclipsed and staggered conformations are found in the crystal structure of [(OEP)MoRu(TPP)]PF₆. The δ -bond strength in **3**⁺ has been estimated as 5.5 kcal/mol using MM2 steric computations.

Acknowledgment. We thank the NSF (Grant CHE 9123187-A4) for financial support. Special thanks to Dr. Doris Hung at Northwestern for mass spectra, Dr. Fred Hollander at the University of California at Berkeley for X-ray data collection, and to Pharmacyclics for their generous gift of diethylpyrrole used in the synthesis of H₂OEP. S.F. and A.P.S. are grateful for the support of a Director's Fellowship at Los Alamos National Laboratory.

Supporting Information Available: Structural information from the X-ray diffraction study of [(OEP)MoRu(TPP)]PF₆ in CIF format, an ESR spectrum of [(OEP)MoRu(OEP)]PF₆, and a solid-state resonance Raman spectrum of [Re(OEP)]₂. This material is available free of charge via the Internet at <http://pubs.acs.org>.

IC981032E